Jihočeská univerzita v Českých Budějovicích
Přírodovědecká fakulta

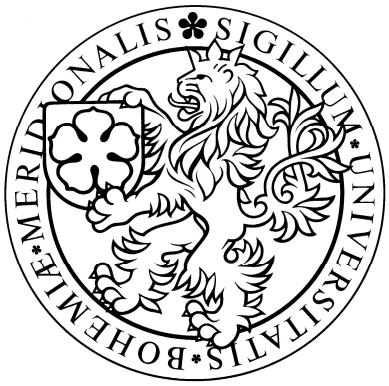

Rigorózní práce

Analysis of the genes of tyrosinkinases KIT and PDGFRα in gastrointestinal stromal tumours

Mgr. Petr Grossmann
České Budějovice, 2007

Grossmann P., 2007: Analysis of the genes of tyrosinkinases KIT and PDGFRα in gastrointestinal stromal tumours. RNDr. thesis, in English] – 14 p., Faculty of Science, University of South Bohemia, České Budějovice, Czech Republic.

Annotation

The study analyse presence and distribution of mutation in gastrointestinal stromal tumours. The alterations were studied in formalin fixed paraffin embeded tissues by temperature gradient gel electrophoresis and sequencing.

Finanční podpora

Tato práce je součástí řešení projektu financovaného grantem Ministerstva zdravotnictví České republiky, MZO 00179906.

Poděkování

Chtěl bych poděkovat prof. MUDr. Bohuslavu Melicharovi, Ph.D. za možnost podílet se na řešení projektu, dále pak RNDr. Tomáši Vaněčkovi, Ph.D. a Mgr. Radku Šímovi za cenné rady v oblasti použitých molekulárně-genetických metod a MUDr. Ondřeji Daumovi a prof. MUDr. Michalovi Michalovi za určení histologických preparátů.

Prohlašuji, že jsem tuto rigorózní práci vypracoval samostatně pouze s použitím citované literatury.

V Plzni, 29. srpna 2007 …….....…..

Autor následujícího článku (Melichar *et al*., Fatal Venous Thrombembolism Complicating Imatinib Therapy in a Patient with Metastatic Gastrointestinal Stromal Tumor, J. Exp. Clin. Cancer Res., 25, 4, 2006, 207-210) potvrzuje, že Mgr. Petr Grossmann přispěl k publikaci této práce provedením molekulárně-genetické analýzy, tj. izolaci DNA z parafínového bloku a analýzou mutací vybraných exonů genů *c-kit* a *PDGFRA*.

prof. MUDr. Bohuslav Melichar, Ph.D. .....

Fatal Venous Thrombembolism Complicating Imatinib Therapy in a Patient with Metastatic Gastrointestinal Stromal Tumor

B. Melichar[1,2], J. Laco[3], L. Slovácek[2], P. Grossmann[4], T. Vanecek[4]

Departments of Oncology & Radiotherapy[1], Medicine[2] and Pathology[3]; Charles University Medical School & Teaching Hospital, Hradec Králové; Department of Pathology[4], Charles University Medical School & Teaching Hospital, Plzen - Czech Republic

Imatinib, a tyrosine kinase inhibitor, is currently the therapy of choice for gastrointestinal stromal tumor (GIST). The toxic effects of imatinib treatment are usually mild, and serious adverse events are rare. We report here the case of a patient with peritoneal metastases of GIST involving the pelvis treated by imatinib. Abdominal pain deteriorated early in the course of the therapy along with the enlargement of the tumors. The patient died suddenly, and the autopsy revealed pulmonary embolism originating from the deep vein thrombosis caused by the compression of common iliac vein by the tumor. The possibility of deep vein thrombosis caused by the compression of the veins by necrotic tumor should be considered in patients with abdominal or pelvic metastases of GIST, including patients treated with imatinib.

Key Words: Gastrointestinal stromal tumor; Imatinib; Venous thrombembolism

Gastrointestinal stromal tumors (GIST) are rare neoplasms characterized by activating mutations of c-kit, or, in the minority of cases, of platelet-derived growth factor receptor-alpha (PDGFRA) (1). Radical surgery is the only curative therapy in GIST, but more than 50% of patients will eventually relapse (2). Liver and peritoneum are the most frequent sites of metastatic disease in GIST. The prognosis of patients with metastatic GIST was, until recently, dismal (2, 3), as resection is feasible only in a small proportion of patients, and GIST represents a chemoresistant tumor (4). The advent of imatinib, a c-kit tyrosine kinase inhibitor, has changed the natural history of metastatic GIST (5). Only 10-20 % of patients initially progress on imatinib (6, 7), and more than 80 % of patients are alive 2 years after the start of treatment (1, 8). Even cases of pathological complete response have been described in GIST after imatinib therapy (9).

Compared to conventional cytotoxic agents, imatinib is, in general, well tolerated (6, 7). The toxicities, including diarrhea or edema, are usually mild. A rare life-threatening side effect, reported solely in patients with GIST, is gastrointestinal or intraperitoneal bleeding secondary to tumor rupture following massive tumor necrosis caused by imatinib (10). This toxicity has been reported in fewer than 5 % of patients, but warrants vigilance, especially in patients presenting with massive intraabdominal metastases or unresected primary tumor. We report here the case of a patient in whom expansion of a necrotic peritoneal GIST metastasis shortly after initiation of imatinib therapy led to venous compression and ileofemoral thrombosis with fatal pulmonary embolism.

Case Description

A 49-year old male presented in February 2004 with abdominal pain. His personal history was remarkable for malignant melanoma in the back that was excised in 1987. In July 2002, axillary lymph node was removed containing metastatic melanoma, and the patient was subsequently treated with adjuvant interferon-α for 3 months. The patient was then followed and was well for the next 12 months.

Since December 2003, the patient complained about abdominal pain. A tumor in the pelvis was detected by CT of the abdomen and pelvis. On March 30, 2004 the patient underwent laparotomy. A large

pelvic tumor reaching to the level of umbilicus was found that was contiguous with distal ileum and adhered to the cecum and peritoneum. The surgical procedures performed included resection of the tumor encompassing ileal resection and partial omentectomy. Because of previous diagnosis of malignant melanoma, the tumor was originally considered metastatic melanoma, but histological examination unexpectedly revealed ileal GIST with diffuse expression of CD34 and focal expression of c-kit (CD117) on immunohistochemical examination. The tumor originated in the distal ileum, and histological examination of resected omentum revealed implantation metastasis of GIST. Although the surgical intervention resulted in substantial reduction of the tumor mass, it was not radical.

The patient was subsequently referred for further therapy. Control CT scan of the abdomen and pelvis on May 5, 2004 revealed persistent pelvic mass 40 x 30 mm, pararectal mass 75 x 45 mm and at least 3 smaller masses around 20 mm. On physical examination, a resistence in the right hypogastrium was observed. Because of the diagnosis of metastatic GIST involving peritoneum, the therapy with imatinib mesylate (400 mg/day) was started on May 27, 2004. At that time the patient complained about the pain in the right hypogastrium. These complaints continued after the start of the therapy. Because of increased severity of the pain, analgesic therapy with transdermal fentanyl was initiated. The patient also reported anorexia, and therapy with oral megestrol acetate suspension was started (800 mg/day). Subsequently, the patient reported pain in the right groin and a resistence in the right thigh. On physical examination, progression of the elastic resistence in the right hypogastrium was noted. Because of continuing complaints, the patient was admitted for observation on June 15, 2004. The patient also reported pain in the left hip. It was suspected that the complaints were caused by expansion of necrotic tumors in the pelvis, and it was feared that a hemorrhage could follow. Subsequently, edema was noted in the left lower extremity and on genitals. Doppler ultrasonographic examination of the veins of lower extremities was performed on June 18. The examination revealed dilatation and slowing of the blood flow in the iliac and femoral veins caused by compression secondary to an expansion in the pelvis, but no signs of venous thrombosis. Antiedematous therapy with prednisone (20 mg/day) was initiated. On June 23, 2004 in the late afternoon hours the patient suddenly lost consciousness. Hypotension was followed by cardiac arrest. Despite cardiopulmonary resuscitation, the patient died 30 minutes later.

The autopsy revealed ileofemoral thrombosis and massive pulmonary embolism that was the immediate cause of death. The left ileofemoral thrombosis was caused by the compression of iliac vein by a large necrotic tumor (Fig. 1). Microscopic examination of the tumor, including immunohistochemistry, revealed GIST with extensive areas of necrosis (Fig. 2). In contrast, no areas of necrosis were evident in the surgical specimen obtained 3 months earlier. Molecular genetic analysis performed on the paraffin blocks from the resection specimen revealed no mutations in exons 9, 11, 13 and 17 of c-kit gene and exons 12, 14 and 18 of PDGFRA gene.

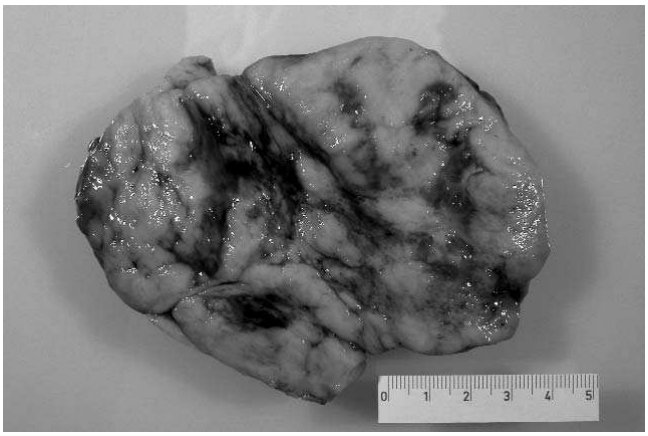

Fig. 1 - Large pelvic tumor that caused the compression of common iliac vein. Areas of hemorrhagic necrosis are evident.

Fig. 2 - Microscopic appearance of metastatic GIST at autopsy (hematoxylin-eosin 100x). Extensive areas of necrosis are evident.

Discussion

Imatinib is currently standard therapy for two relatively rare neoplastic disorders: chronic myeloid leukemia and GIST. In both diseases, imatinib represents an effective and relatively well-tolerated drug. Most common toxicities of imatinib therapy include mild diarrhea and edema, but these side effects rarely warrant therapy, or a dose reduction. Hemorrhage subsequent to massive tumor necrosis and tumor rupture is a rare, but potentially fatal complication of imatinib therapy that is specific for GIST (10). This complication was also suspected in the present patient. Abdominal pain and sudden loss of consciousness with hypotension may be suggestive of intraabdominal hemorrhage from a ruptured necrotic tumor. In the present case, however, these symptoms accompanied ileofemoral thrombosis that was caused by the compression of common iliac vein by a largely necrotic tumor and to fatal pulmonary embolism.

Thrombembolic disease is a common complication in cancer patients. Three basic mechanisms have been defined in the 19th century by Virchow to be the cause of venous thrombosis: decrease of blood flow, injury to the vessel wall and disturbances in the balance between procoagulant and anticoagulant factors (11). Although in most cancer patients thrombosis may be caused by the disturbed balance between procoagulant and anticoagulant activity (12), the deep vein thrombosis that resulted in fatal pulmonary embolism in the present case was evidently caused to a larger part by local factors, i.e. compression of the common iliac vein and slowing of venous flow. It is, however, possible only to speculate whether the massive tumor necrosis that lead to the iliac vein compression and thrombosis was merely result of only spontaneous process that is common in GIST, or whether was the necrosis caused and increased by the administration of imatinib. A marked increase in tumor necrosis observed at autopsy compared to no areas of necrosis in the resection specimen of similar size as the recurrent tumor could point to the latter. No mutation in the c-kit or PDGFRA genes was found in the tumor specimen in the present case. Tumors without c-kit or PDGFRA mutations represent a minority of GIST cases (1, 13). Partial response to imatinib therapy has been documented in these cases, although the probability of response is substantially lower than in tumors harboring c-kit or PDGFRA mutations (13). In any case, the possibility of the compression of the large veins associated with tumor necrosis should be considered in patients with pelvic metastases of GIST treated with imatinib. The present case demonstrates that not only intraabdominal hemorrhage, but also thrombembolic disease may complicate the early phase of the therapy of metastatic GIST with imatinib, and the possibility of thrombembolic disease should be considered in the differential diagnosis in patients with metastatic GIST, including those treated with imatinib, presenting with acute complaints.

In conclusion, in the present report we describe thrombembolic disease as a rare, but potentially fatal complication of imatinib therapy. The possibility of deep vein thrombosis caused by the compression of the veins by necrotic tumor should be considered in patients with abdominal or pelvic metastases of GIST treated with imatinib.

Acknowledgement: Supported by Research Project of the Ministry of Health of the Czech Republic MZO 00179906.

References

1. Heinrich M.C., Corless C.L., Demetri G.D., et al. : Kinase mutations and imatinib response in patients with metastatic gastrointestinal stromal tumor. J. Clin. Oncol. 21: 4342 - 4349, 2003.
2. Crosby J.A., Catton C.N., Davis A., et al. : Malignant gastrointestinal stromal tumors of the small intestine: a review of 50 cases from a prospective database. Ann. Surg. Oncol. 8: 50 - 59, 2001.
3. DeMatteo R.P., Lewis J.J., Leung D., Mudan S.S., Woodruff J.M., Brennan M.F.: Two hundred gastrointestinal stromal tumors. Recurrence patterns and prognostic factors for survival. Ann. Surg. 231: 51 - 58, 2000.
4. DeMatteo R.P., Heinrich M.C., El-Rifai W.M., Demetri G.: Clinical management of gastrointestinal stromal tumors: before and after STI-571. Human Pathol. 33: 466 - 477, 2002.
5. Fiorentini G., Bernardesci P., De Simone M., et al. : Efficacy of imatinib mesylate in patients with liver metastases from gastrointestinal stromal tumor failing intra-arterial hepatic chemotherapy with epirubicin. J. Exp. Clin. Cancer Res. 22 (Supplement): 13 - 16, 2003.
6. Demetri G.D., von Mehren M., Blanke C.D., et al. : Efficacy and safety of imatinib mesylate in advanced gastrointestinal stromal tumors. N. Engl. J. Med. 347: 472 - 480, 2002.
7. van Oosterom A.T., Judson I., Verweij J., et al. : Safety and efficacy of imatinib (STI571) in metastatic gastrointestinal stromal tumours: a phase I study. Lancet 358: 1421 - 1423, 2001.
8. Wu P.C., Langerman A., Ryan C.W., Hart J., Swiger S., Posner M.C.: Surgical treatment of gastrointestinal stromal tumors in the imatinib (STI-571) era. Surgery 134: 656 - 666, 2003.
9. Melichar B., Voboril Z., Nozicka J., et al. : Pathological complete response in advanced gastrointestinal stromal tumor after imatinib therapy. Intern. Med. 44: 1163 - 1168, 2005.

10. Reichardt P., Schneider U., Stroszczynski C., Pink D., Hohenberger P.: Molecular response of gastrointestinal stromal tumour after treatment with tyrosine kinase inhibitor imatinib mesylate. J. Clin. Pathol. 57: 215 - 217, 2004.
11. Kyrle P.A., Elchinger S.: Deep vein thrombosis. Lancet 365: 1163 - 1174, 2005.
12. Goldenberg N., Kahn S.R., Salymass S.: Markes of coagulation and angiogenesis in cancer-associated venous thromboembolism. J. Clin. Oncol. 21: 4194 - 4199, 2003.
13. Debiec-Rychter M., Dumez H., Judson B., et al. : Use of c-KIT/PDGFRA mutational analysis to predict the clinical response to imatinib in patients with advanced gastrointestinal stromal tumours entered on phase I and II studies of the EORTC Soft Tissue and Bone Sarcoma Group. Eur. J. Cancer 40: 689 - 695, 2004.

Received:April 12 , 2006

Bohuslav Melichar M.D., Ph.D.
Department of Oncology & Radiotherapy,
Charles University Medical School & Teaching Hospital,
Sokolská 581, Building 23, 500 05
Hradec Králové, Czech Republic
phone: +420-49-582149, fax: +420-49-5832081,
e-mail: melichar@fnhk.cz

Korespondující autor následujícího článku (Daum *et al.*, Diagnostic morphological features of PDGFRA-mutated gastrointestinal stromal tumors: molecular genetic and histologic analysis of 60 cases of gastric gastrointestinal stromal tumors, Annals of Diagnostic Pathology, 11 (2007), 27–33) Prof. MUDr. Michal Michal potvrzuje, že Mgr. Petr Grossmann přispěl velkou měrou k publikaci této práce. Provedl převážnou část molekulárně-genetických analýz, a to výběr a shromáždění vzorků, izolace DNA z parafínových bloků, návrh a modifikaci primerů pro některé exony genů *c-kit* a *PDGFRA*, skríning mutací TGGE heteroduplexovou analýzou, reamplifikaci a sekvenaci pozitivních vzorků s predikcí aberantních proteinů.

Prof. MUDr. Michal Michal .....

Available online at www.sciencedirect.com
ScienceDirect
Annals of Diagnostic Pathology 11 (2007) 27–33
Annals of DIAGNOSTIC PATHOLOGY

Diagnostic morphological features of *PDGFRA*-mutated gastrointestinal stromal tumors: molecular genetic and histologic analysis of 60 cases of gastric gastrointestinal stromal tumors

Ondrej Daum, MD, Petr Grossmann, MD, Tomas Vanecek, MSc, Radek Sima, MSc, Petr Mukensnabl, MD, Michal Michal, MD*

Department of Pathology, Medical Faculty Hospital, Charles University, Plzen, Czech Republic

Abstract In this study, 60 gastrointestinal stromal tumors of the stomach were analyzed to elucidate the possible relation of their morphology to the mutation status of *KIT* and *PDGFRA* genes. The patients included 27 men and 33 women with a mean age of 63.8 years (range, 12-92 years). Only 1 tumor occurred before the age of 21 years. *KIT* mutations were detected in 31 cases (51.7%), *PDGFRA* mutations in 22 cases (36.7%), and 7 cases (11.7%) were *KIT* and *PDGFRA* wild type. When the mutation status was correlated with histologic features of the tumors, epithelioid or mixed epithelioid/spindle cell pattern and mast cell infiltration were found as the most reliable signs of *PDGFRA* mutation. Neoplastic rhabdoid cells and multinucleated giant cells, also previously reported as features of *PDGFRA*-mutated gastrointestinal stromal tumors, seemed to be less specific but still helpful markers in our study. Finally, tumor-infiltrating lymphocytes and myxoid stroma do not seem to be valuable histologic signs.

Keywords: GIST; Stromal tumor; KIT; PDGFRA; Morphology

1. Introduction

Gastrointestinal stromal tumors (GISTs), originally classified among smooth muscle tumors [1], are now viewed as a spectrum of mesenchymal neoplasms differentiating toward the phenotype of interstitial cells of Cajal. They represent the most common mesenchymal tumors of the gastrointestinal tract, the stomach being the most prevalent site of occurrence; however, they can also occur, albeit rarely, in the gallbladder [2,3], pancreas [4,5], urinary bladder serosa [6], and even the vagina [7]. In 1998, expression of KIT protein [8], as well as c-kit "gain of function" mutations [9], was proved to be a diagnostic sign and important pathogenetic event in GIST tumorigenesis. However, a subset of morphologically indubitable GISTs remained KIT immunonegative and c-kit wild type. In 2003, activating mutations of *PDGFRA* (platelet-derived growth factor receptor α) were detected in a significant portion of these KIT-negative GISTs [10,11]. Since then, *PDGFRA*-mutated GISTs were shown to posses several possible morphological signs distinguishing them from c-kit–mutated tumors at the light microscopic level, namely, epithelioid pattern [12-15], myxoid stroma [16], tumor-infiltrating mast cells [16], tumor-infiltrating lymphocytes [17], giant multinucleated neoplastic cells [18], and rhabdoid cells [17].

The purpose of this study was to evaluate the relation of all these promising markers to the mutational status of c-kit and *PDGFRA* in a series of 60 gastric GISTs.

2. Materials and methods

Sixty specimens of GISTs were retrieved from 200 patients with GISTs accessed from Sikl's Department of Pathology, Charles University, and from one of the authors (MM) as referral cases during the last 10 years. Tissues for light microscopy were fixed in 4% formaldehyde and embedded in paraffin using routine procedures. Five-micrometer-thick sections were cut from the tissue blocks and stained with hematoxylin-eosin.

* Corresponding author. Department of Pathology, Laborator Spec. Diagnostiky, Medical Faculty Hospital, Plzen 323 18, Czech Republic. Tel.: +420 603886633; fax: +420 377104650.
E-mail address: michal@medima.cz (M. Michal).

1092-9134/$ – see front matter © 2007 Elsevier Inc. All rights reserved.
doi:10.1016/j.anndiagpath.2006.10.002

Table 1
Basic patterns of GISTs according to Miettinen et al [19]

1. Spindle cell GISTs	2. Epithelioid GISTs
A. Sclerosing	A. Sclerosing syncytial
B. Palisading and vacuolated	B. Dyscohesive
C. Hypercellular	C. Hypercellular
D. Sarcomatous	D. Sarcomatous

The tumors were then classified to basic patterns according to Miettinen et al [19] as shown in Table 1. Furthermore, the slides were evaluated for the presence of multinucleated giant cells, rhabdoid cells, tumor-infiltrating lymphocytes and mast cells, and edematous to myxoid stroma. We did not discern between stromal edema and true myxoid change because these 2 terms are used interchangeably in the literature, and, in fact, some of the previous reports possibly designate stromal edema as myxoid change of the stroma. Mast cells were visualized using immunohistochemical stain for mast cell tryptase as shown below.

Primary antibodies used for immunohistochemical investigations are summarized in Table 2. The primary antibodies were visualized using the supersensitive streptavidin-biotin-peroxidase complex (BioGenex, San Ramon, Calif). Appropriate positive and negative control slides were used.

DNA for molecular genetic investigation was extracted from formalin-fixed, paraffin-embedded tissues. Several 5-μm-thick sections were placed on the slides. Hematoxylin and eosin–stained slides were examined for determination of area of tumor tissue. Then, tumor tissue from unstained slides was scraped and DNA was isolated using the DNeasy Tissue Kit (QIAgen, Hilden, Germany) according to the manufacturer's protocol. In several cases, where quality or amount of extracted DNA was low, concentration with Microcon 100 (Millipore, Billerica, Mass) according to the manufacturer's protocol was carried out.

Mutational analysis of exons 9, 11, 13, and 17 of the c-kit gene (accession number U63834) and exons 12, 14, and 18 of the *PDGFRA* gene (accession number D50017) was performed using PCR and direct sequencing.

Polymerase chain reaction (PCR) was carried out using the primers shown in Table 3. The reaction conditions were as follows: 12.5 μL of HotStart Taq PCR Master Mix (QIAgen, Hilden, Germany), 10 pmol of each primer, 100 ng of template DNA, and distilled water up to 25 μL. The amplification program consisted of denaturation at 95°C for 15 minutes and then 40 cycles of denaturation at 95°C for 1 minute, annealing at 55°C for 1 minute and extension at 72°C for 1.5 minutes for all amplicons. The program was finished by 72°C incubation for 7 minutes.

Table 3
Polymerase chain reaction primers used in the study

Gene/exons	Name	Primers
c-kit exon 9a[a,b]	c-kit e9aNF	GAGTAAGCCAGGGCTTTTGTT
	c-kit e9aNR	CGTGCCATTGTGCTTGAAT
c-kit exon 9b[b,c]	c-kit e9bNF	CCGTTTGGAAAGCTAGTGGT
	c-kit e9bNR	CAGAGCCTAAACATCCCCTTA
c-kit exon 11	c-kit e11NF	TGTTCTCTCTCCAGAGTGCTCTAA
	c-kit e11NR	ACCCAAAAAGGTGACATGGA
c-kit exon 13	c-kit e13F	CATGCGCTTGACATCAGTTT
	c-kit e13R	CAATAAAAGGCAGCTTGGACA
c-kit exon 17[b]	c-kit e17WF	ATGGTTTTCTTTTCTCCTCC
	c-kit e17WR	TACATTATGAAAGTCACAGG
PDGFRA exon 12[b]	PDG e12F	CTCTGGTGCACTGGGACTTT
	PDG e12R	GGAGGTTACCCCATGGAACT
PDGFRA exon 14	PDG e14F	GCTCAGCTGGACTGATATGTGA
	PDG e14R	CCAGTGAAAATCCTCACTCCA
PDGFRA exon 18[b]	PDG e18F	GCTACAGATGGCTTGATCCTG
	PDG e18R	GACCAGTGAGGGAAGTGAGG

[a] 5′ end of exon 9.
[b] See Ref. [20].
[c] 3′ end of exon 9.

Successfully amplified PCR products were purified with a Montage PCR Centrifugal Filter Device (Millipore, Billerica, Mass); both sides were sequenced using a Big Dye Terminator Sequencing kit (PE/Applied Biosystems, Foster City, Calif) and run on an automated sequencer ABI Prism 310 (PE/Applied Biosystems) at a constant voltage of 11.3 kV for 20 minutes.

3. Results

The clinical features and mutation status of studied GISTs are shown in Table 4. The patients included 27 men and 33 women with a mean age of 63.8 years (range, 12-92 years). Only 1 tumor occurred before the age of 21 years. The size of tumors was known in 52 cases. In these, tumor size varied

Table 2
Primary antibodies used in the study

Antibody	Clone	Dilution	Pretreatment	Manufacturer
Vimentin	V9	1:800	Microwave	Neomarkers, Fremont, Calif
CD117	Polyclonal	1:100	0	Dako, Glostrup, Denmark
CD34	QBEnd/10	1:800	0	Neomarkers
Smooth muscle actin	1A4	1:1000	0	Dako
Muscle-specific actin	HHF35	1:3000	0	Dako
Desmin	D33	1:300	0	Dako
S-100 protein	Polyclonal	1:200	0	Dako
Pankeratin	AE1/AE3	1:1000	Microwave	Neomarkers
Low molecular weight cytokeratin	CAM 5.2	1:50	Microwave	Becton Dickinson, San Jose, Calif
Epithelial membrane antigen	E29	1:700	0	Dako
Mast cell tryptase	AA1	1:250	Pepsin	Dako
Ki-67 antigen	MIB1	1:1000	Microwave	Dako

Table 4
Clinical features and mutation status

Case	Sex	Age	Diameter	Mutations
1	F	71	3.5 cm	E11 c-kit (V559D)
2	M	80	3 cm	E18 PDGFRA (D842V)
3	F	59	0.9 cm	E11 c-kit (V560D)
4	F	63	8.5 cm	E11 c-kit (R586-N587insTQLPYDHKWEFPR)[a]
5	M	44	19 cm	E11 c-kit (W557_K558del)
6	F	43	7 cm	wt
7	F	63	5 cm	E14 PDGFRA (N659K)
8	F	54	<2 cm	E11 c-kit (V559G)
9	M	48	2.5 cm	E18 PDGFRA (D842V)
10	M	61	4 cm	E12 PDGFRA (V561D)
11	M	62	7 cm	wt
12	M	79	9 cm	E11 c-kit (W557R)
13	M	74	9 cm	E11 c-kit (V559del)
14	F	82	7 cm	E11 c-kit (V559D)
15	F	47	14 cm	wt
16	F	70	Multiple, largest 10 cm	wt
17	M	71	0.8 cm	E11 c-kit (V560E)
18	F	81	4.5 cm	E11 c-kit (V559D)
19	M	41	3 cm	E11 c-kit (P585-R586insTQLPYDHKWEFP)[a]
20	F	77	3 cm	E11 c-kit (W557_K558del)
21	M	66	4 cm	E12 PDGFRA (V561D)
22	M	92	1.5 cm	E11 c-kit (L576P)
23	M	77	NAV	E11 c-kit (L589-S590insPYDHKWEFPRNRL)[a]
24	F	29	NAV	E18 PDGFRA (D842_H845del)
25	M	83	5 cm	E13 c-kit (K642E)
26	F	76	18 cm	E11 c-kit (W557_K558del)
27	F	63	12 cm	E18 PDGFRA (D842_H845del)
28	M	70	0.7 cm	E11 c-kit (W557_K558del)
29	M	54	0.5 cm	E11 c-kit (Y553_W557del)
30	F	62	3 cm	E11 c-kit (M552_W557del)
31	F	55	"Large"	E11 c-kit (K550_K558del)
32	F	69	2.5 cm	E18 PDGFRA (D842_H845del)
33	M	52	1.5 cm	E18 PDGFRA (D842_H845del)
34	M	52	8 cm	E18 PDGFRA (D842V)
35	M	60	NAV	E11 c-kit (V569_Q575delinsE)
36	F	71	4.5 cm	E12 PDGFRA (S566_E571delinsR)
37	F	77	14 cm	E11 c-kit (W557_K558del)
38	F	74	6 cm	E11 c-kit (W557G)
39	M	74	10 cm	E11 c-kit (Q556_V559delinsPF)
40	M	73	7 cm	E18 PDGFRA (D842V)
41	F	63	NAV	wt
42	F	12	NAV	wt
43	M	44	NAV	E11 c-kit (K558_P573delinsR)
44	F	48	Multiple, largest 6 cm	wt
45	M	75	2.5 cm	E18 PDGFRA (D842V)
46	M	69	4.5 cm	E18 PDGFRA (D842V)
47	M	62	8 cm	E11 c-kit (W557_K558del)
48	M	59	6 cm	E18 PDGFRA (D842V)
49	M	74	0.5 cm	E11 c-kit (Y578-D579insPY)[a]
50	F	63	4 cm	E11 c-kit (W557R)
51	F	53	3 cm	E11 c-kit (P551_Q556delinsHV)
52	F	69	4.5 cm	E11 c-kit (V559A)
53	F	70	11 cm	E11 c-kit (V559D)
54	F	77	4 cm	E12 PDGFRA (F565-S566insRIRWRVIESI)[b]
55	F	60	12 cm	E18 PDGFRA (M844_S847delinsP)
56	F	53	3 cm	E18 PDGFRA (D842V)
57	F	63	10 cm	E18 PDGFRA (D842V)
58	F	76	3 cm	E18 PDGFRA (D842V)
59	M	60	4.5 cm	E18 PDGFRA (D842V)
60	F	76	NAV	E18 PDGFRA (D842V)

M indicates male; F, female; wt, wild type.
[a] Duplication.
[b] Substitution/duplication.

Table 5
Histologic findings

Case	CD117	Pattern[a]	Mast cells	TILs[b]	Myxoid stroma	Rhabdoid cells	Giant cells
1	+	1c	–	+	–	–	–
2	–	2a/2b	+	+	+	+	–
3	+	1a	–	+	–	–	–
4	+	2b	–	–	–	+	+
5	+	1c	–	–	–	–	–
6	–	1c/2b	–	+	+	+	+
7	+	2a/2b	+	+	+	+	+
8	–	1b	–	–	+	–	–
9	+	2b	+	+	+	+	+
10	–	1b/2b	+	+	+	+	+
11	+	1b	–	–	+	–	–
12	+	1b	–	+	–	–	–
13	+	1b	–	+	–	–	–
14	+	2a/2b	–	+	+	+	+
15	–	2a/2b	+	+	+	+	–
16	+	1b	–	+	+	–	–
17	+	1b	–	–	+	–	–
18	+	1b	–	–	–	–	–
19	+	1b	–	+	+	+	+
20	+	1c	–	+	–	–	–
21	+	2b	+	+	+	+	+
22	+	1a/1b	–	–	+	–	–
23	+	1c/2c	–	–	+	+	–
24	–	2c	–	+	–	+	–
25	+	1b/1c	–	–	+	–	–
26	+	1c	–	+	+	+	–
27	+	2c	+	+	+	+	+
28	–	1a	–	–	–	–	–
29	–	1a	–	–	–	–	–
30	+	1b	–	–	+	–	–
31	+	1b	–	–	+	–	+
32	–	2a/2b	+	+	–	+	–
33	–	1b/2b	–	–	–	–	–
34	+	1b/2b	+	+	+	–	+
35	+	1b	–	+	–	–	–
36	–	2b	+	+	–	–	–
37	+	1c	–	+	–	+	+
38	+	1b	–	+	–	–	–
39	+	1b	–	–	–	–	–
40	–	2c	+	+	–	–	–
41	+	1c	–	+	–	–	–
42	+	1c/2c	–	+	–	–	–
43	+	1d	–	–	+	–	–
44	+	2b/2c	–	–	+	+	+
45	–	2a/2b	+	+	+	–	–
46	+	2a/2b	+	+	+	+	+
47	+	1c	–	–	–	–	–
48	–	2a/2b	+	+	+	+	+
49	+	1a	–	–	–	–	–
50	+	1b/2b	–	+	–	–	–
51	+	1b	–	+	–	–	–
52	+	1b	–	+	+	–	–
53	+	1b	–	+	+	–	–
54	+	2b	+	–	+	–	–
55	–	2b	+	–	+	–	+
56	–	2b	+	+	+	+	+
57	–	2c	+	+	+	+	+
58	–	2a/2b	–	+	–	+	+
59	–	2b	+	+	–	+	+
60	–	2b	+	+	+	+	–

[a] Pattern according to Miettinen et al [19] (Table 1).
[b] Tumor-infiltrating lymphocytes.

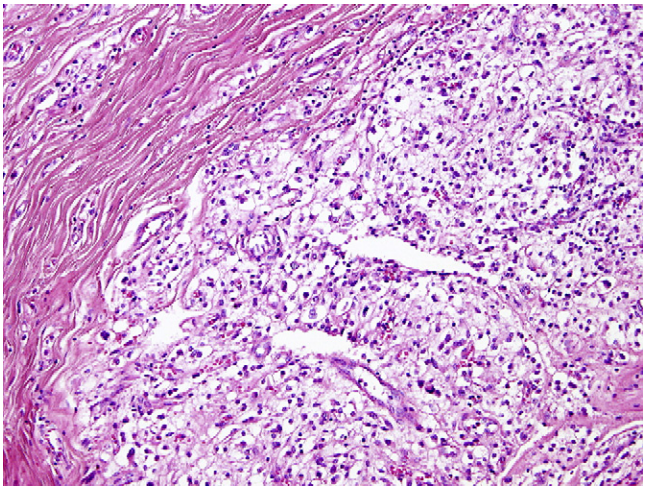

Fig. 1. Epithelioid pattern of *PDGFRA*-mutated GIST.

from 0.5 to 19 cm (mean, 5.9 cm). In total, 31 tumors were found to be c-kit mutated, 22 *PDGFRA* mutated, and 7 tumors to be wild type. *KIT* exon 11 mutations were detected in 30 cases (50%), *KIT* exon 13 mutation in 1 case (1.7%), *PDGFRA* exon 18 mutations in 17 cases (28.3%), *PDGFRA* exon 12 mutations in 4 cases (6.7%), and *PDGFRA* exon 14 mutation in 1 case (1.7%). Seven cases (11.7%) were *KIT* and *PDGFRA* wild type. The average diameter of *KIT*-mutated tumors was slightly higher than that of *PDGFRA*-mutated GISTs (5.9 and 5.1 cm, respectively). Whereas male/female ratio was almost equal in *KIT*- and *PDGFRA*-mutated GISTs (15/16 and 11/11, respectively), female sex significantly prevailed in wild-type tumors (1/6).

All the tumors were positively stained with antibody against vimentin. Smooth muscle actin, muscle-specific actin, desmin, S-100 protein, CD34, pankeratin, and low molecular weight cytokeratin were positive in 13, 4, 2, 3, 45, 9, and 2 cases, respectively (exact data not shown).

Histologic features evaluated as possible signs for discriminating between *KIT*- and *PDGFRA*-mutated GISTs

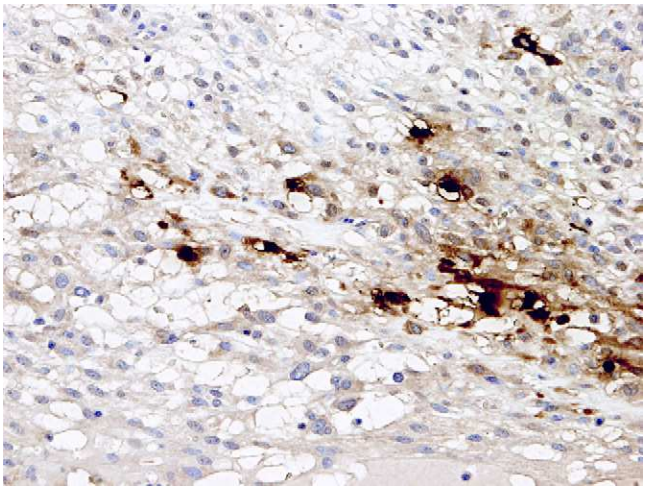

Fig. 2. Tumor-infiltrating mast cells in *PDGFRA*-mutated GIST (mast cell tryptase).

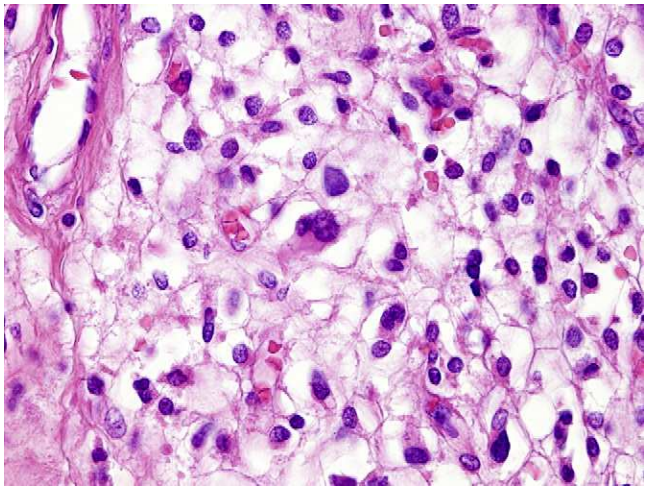

Fig. 3. Multinucleated giant cells were less specific signs of GISTs with *PDGFRA* mutation.

are shown in Table 5. As for KIT immunoexpression, CD117 was negative in 20 cases. Of these, 15 cases were *PDGFRA* mutated, 3 *KIT* mutated, and 2 wild type. In the group of *PDGFRA*-mutated tumors, 15 were CD117 negative and 7 were CD117 positive. Thirty tumors displayed epithelioid or mixed spindle/epithelioid cell pattern (Fig. 1). Of these, 73.3% were *PDGFRA* mutated, 13.3% *KIT* mutated, and 13.3% *KIT* and *PDGFRA* wild type. Foci of so-called myxoid stroma were found in 33 cases. Of these, 37.5% were *KIT* mutated, 46.9% *PDGFRA* mutated, and 15.6% *KIT* and *PDGFRA* wild type. Intratumoral mast cells were highlighted by antibody against mast cell tryptase in 20 cases (Fig. 2); none of them were *KIT* mutated, 95% carried *PDGFRA* mutation, and 5% were wild type. Multinucleated giant neoplastic cells were present in 20 cases (Fig. 3). Of these, 25% were *KIT* mutated, 65% *PDGFRA* mutated, and 10% *KIT* and *PDGFRA* wild type. Tumor-infiltrating lymphocytes were

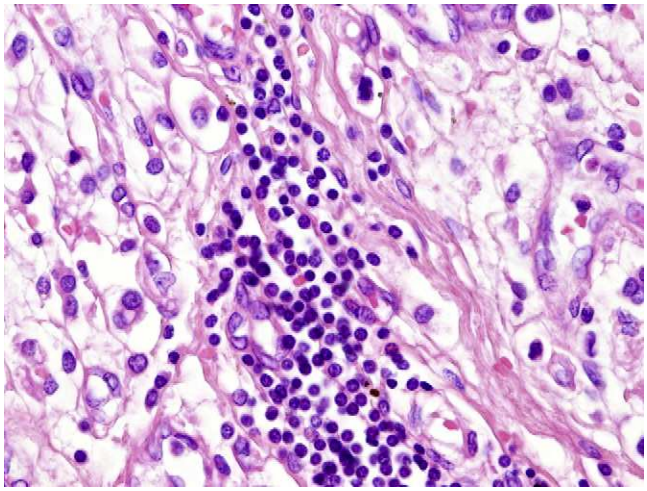

Fig. 4. Tumor-infiltrating lymphocytes did not prove to be useful a histological marker for discriminating between *KIT* and *PDGFRA* mutation.

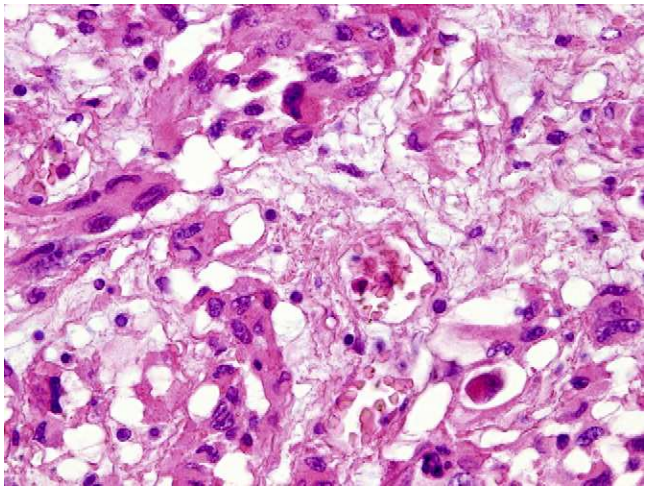

Fig. 5. Rhabdoid cells, multinucleated giant cells, myxoid stroma, and epithelioid pattern are often seen together in hematoxylin and eosin–stained slides of *PDGFRA*-mutated GISTs.

detected in 39 cases (Fig. 4), 38.5% of which were *KIT* mutated, 48.7% carried *PDGFRA* mutation, and 12.8% were wild type. Finally, rhabdoid neoplastic cells were identified in 24 tumors (Fig. 5). Of these, 25% were *KIT* mutated, 62.5% *PDGFRA* mutated, and 12.5% *KIT* and *PDGFRA* wild type.

Thus, the presence of epithelioid component and mast cell intratumoral infiltration seems to be the most powerful histologic feature distinguishing *KIT*- and *PDGFRA*-mutated GISTs (Table 6). This is further supported by comparison of occurrence of studied histologic features in *PDGFRA*-mutated and *PDGFRA* wild-type groups of GISTs (Table 7), which shows epithelioid pattern and intratumoral mast cells as the most potent predictors of *PDGFRA* mutation.

4. Discussion

As mutations of the *PDGFRA* gene had been detected in a subset of GISTs [10,11], several studies on histologic characteristics of this subtype of GISTs were published. These studies offered some morphological signs distinguishing *PDGFRA*-mutated from c-kit–mutated tumors at the light microscopic level, namely, epithelioid pattern [12-15], myxoid stroma [16], tumor-infiltrating mast cells [16], tumor-infiltrating lymphocytes [17], giant multinucleated neoplastic cells [18], and rhabdoid cells [17].

In this study, we reviewed 60 cases of gastric GISTs for mutations in exons 9, 11, 13, and 17 of c-kit, and exons 12, 14, and 18 of *PDGFRA* genes. We also evaluated the relation of these mutations to the above-mentioned histologic features.

Of the 60 tumors, 31 cases were found to be c-kit mutated, 22 *PDGFRA* mutated, and 7 tumors wild type. *KIT* exon 11 mutations were detected in 30 cases (50%), *KIT* exon 13 mutation in 1 case (1.7%), *PDGFRA* exon 18 mutations in 17 cases (28.3%), *PDGFRA* exon 12 mutations in 4 cases (6.7%), and *PDGFRA* exon 14 mutation in 1 case (1.7%). Thus, the vast majority of PDGFRA mutations clustered in the TK II domain, and of these, all but one affected codon 842. D842V missense mutation was particularly common and represented 70.6% of all PDGFRA exon 18 mutations. Seven cases (11.7%) were *KIT* and *PDGFRA* wild type. These results are in good concordance with previous reports when referred to specific locations. Namely, the high frequency of *PDGFRA* exon 18 mutations and rarity of *KIT* exon 9 mutations in gastric GISTs reported previously [13-15] were confirmed by this study.

Furthermore, we investigated clinicopathologic signs possibly distinguishing *KIT* and *PDGFRA*-mutated GISTs. Both groups showed similar sex distribution with no sex predilection and average size (5.9 and 5.1 cm, respectively). However, we found some histologic features as valuable predictors of the most probable mutation in GIST. As shown in Tables 6 and 7, the most powerful signs of *PDGFRA* mutations are tumor-infiltrating mast cells (in our study highlighted by an antibody against mast cell tryptase) and the presence of an epithelioid component of the tumor. In fact, we found no mast cells in any of the *KIT*-mutated tumors. The predominant epithelioid pattern of *PDGFRA*-mutated GISTs was repeatedly reported before [12-15]. Sakurai et al [16] also reported on mast cell infiltrations in GISTs, the finding confirmed by our study. However, association of myxoid stroma with *PDGFRA* mutation as reported in the same paper was not found in our study. Although the myxoid change may be striking in some cases of *PDGFRA*-mutated GISTs, it does not reliably exclude possible mutations of c-kit. The same is true for the presence of tumor-infiltrating lymphocytes in *PDGFRA*-mutated GISTs reported at the poster section of the Annual Meeting of USCAP in 2006 [17]. On the other hand, rhabdoid

Table 6
Distribution of different mutations according to investigated histologic features

Histologic feature (100%)	*KIT*	*PDGFRA*	wt
Epithelioid component	13.3%	73.3%	13.3%
Myxoid stroma	37.5%	46.9%	15.6%
Mast cells	0	95%	5%
Multinucleated cells	25%	65%	10%
TILs	38.5%	48.7%	12.8%
Rhabdoid cells	25%	62.5%	12.5%

TILs indicates tumor-infiltrating lymphocytes.

Table 7
Occurrence of investigated histologic features in *PDGFRA*-mutated and *PDGFRA* wild-type GISTs

Histologic feature	Non-*PDGFRA* (100%)	*PDGFRA* (100%)
Epithelioid component	20.8%	100%
Myxoid stroma	46.8%	68.2%
Mast cells	2.6%	86.5%
Multinucleated cells	18.2%	59.5%
TILs	52%	86.5%
Rhabdoid cells	23.4%	68.2%

neoplastic cells presented at the same poster [17] and giant multinucleated neoplastic cells reported by Pauls et al [18] were found to be quite useful in discriminating features in our study, although not as sensitive and specific as the epithelioid pattern and tumor-infiltrating mast cells.

In conclusion, we found mast cell infiltration and epithelioid or mixed pattern, followed by presence of rhabdoid and multinucleated giant cells, as the most powerful markers for discriminating between *PDGFRA*- and *KIT*-mutated GISTs, thus enabling time and money saving when focusing on molecular genetic investigation of GISTs.

References

[1] Golden T, Stout AP. Smooth muscle tumours of the gastrointestinal tract and retroperitoneal tissues. Surg Gynecol Obstet 1941;73:784-90.

[2] Mendoza-Marin M, Hoang MP, Albores-Saavedra J. Malignant stromal tumor of the gallbladder with interstitial cells of Cajal phenotype. Arch Pathol Lab Med 2002;126:481-3.

[3] Ortiz-Hidalgo C, Bojorge BL, Albores-Saavedra J. Stromal tumor of the gallbladder with phenotype of interstitial cells of Cajal. A previously unrecognized neoplasm. Am J Surg Pathol 2000;24:1420-3.

[4] Daum O, Klecka J, Ferda J, Treska V, Vanecek T, Sima R, et al. Gastrointestinal stromal tumor of the pancreas: case report with documentation of KIT gene mutation. Virchows Arch 2005;446:470-2.

[5] Neto MRM, Machuca TN, Pinho RV, Yuasa LD, Bleggi-Torres LF. Gastrointestinal stromal tumor: report of two unusual cases. Virchows Arch 2004;444:594-6.

[6] Lasota J, Carlsson JA, Miettinen M. Spindle cell tumor of urinary bladder serosa with phenotypic and genotypic features of gastrointestinal stromal tumor. A clinical report with documentation of KIT expression and mutation. Arch Pathol Lab Med 2000;124:894-7.

[7] Ceballos KM, Francis JA, Mazurka JL. Gastrointestinal stromal tumor presenting as a recurrent vaginal mass. Arch Pathol Lab Med 2004; 128:1442-4.

[8] Sarlomo-Rikala M, Kovatich AJ, Barusevivius A, Miettinen M. CD117: a sensitive marker for a gastrointestinal stromal tumor that is more specific than CD34. Mod Pathol 1998;11:728-34.

[9] Hirota S, Isozaki K, Moriyama Y, Hashimoto K, Nishida T, Ishiguro S, et al. Gain-of-function mutations of c-kit in human gastrointestinal stromal tumors. Science 1998;279:577-80.

[10] Heinrich MC, Corless CL, Duensing A, McGreevey L, Chen CJ, Joseph N, et al. PDGFRA activating mutations in gastrointestinal stromal tumors. Science 2003;299:708-10.

[11] Hirota S, Ohashi A, Nishida T, Isozaki K, Kinoshita K, Shinomura Y, et al. Gain-of-function mutations of platelet-derived growth factor receptor α gene in gastrointestinal stromal tumors. Gastroenterology 2003;125:660-7.

[12] Debiec-Rychter M, Wasag B, Stul M, De Wever I, Van Oosterom A, Hagemeijer A, et al. Gastrointestinal stromal tumours (GISTs) negative for KIT (CD117 antigen) immunoreactivity. J Pathol 2004; 202:430-8.

[13] Lasota J, Dansonka-Mieszkowska A, Sobin LH, Miettinen M. A great majority of GISTs with PDGFRA mutations represent gastric tumors of low or no malignant potential. Lab Invest 2004;84:874-83.

[14] Penzel R, Aulmann S, Moock M, Schwarzbach M, Rieker RJ, Mechtersheimer G. The location of KIT and PDGFRA gene mutations in gastrointestinal stromal tumours is site and phenotype associated. J Clin Pathol 2005;58:634-9.

[15] Wardelmann E, Hrychyk A, Merkelbach-Bruse S, Pauls K, Goldstein J, Hohenberger P, et al. Association of platelet-derived growth factor receptor α mutations with gastric primary site and epithelioid or mixed cell morphology in gastrointestinal stromal tumors. J Mol Diagn 2004;6:197-204.

[16] Sakurai S, Hasegawa T, Sakuma Y, Takazawa Y, Motegi A, Nakajima T, et al. Myxoid epithelioid gastrointestinal stromal tumor (GIST) with mast cell infiltrations: a subtype of GIST with mutations of platelet-derived growth factor receptor alpha gene. Hum Pathol 2004;35: 1223-30.

[17] Kwon J, Kang HJ, Kim H, Kim SEH, Kim H. Different histopathological features between gastrointestinal stromal tumors with KIT and PDGFRA mutation. AbstractLab Invest 2006;86: (Suppl 1):111A.

[18] Pauls K, Merkelbach-Bruse S, Thal D, Büttner R, Wardelmann E. PGFRα- and c-kit mutated gastrointestinal stromal tumours (GISTs) are characterized by distinctive histological and immunohistochemical features. Histopathology 2005;46:166-75.

[19] Miettinen M, Sobin LH, Lasota J. Gastrointestinal stromal tumors of the stomach. A clinicopathologic, immunohistochemical, and molecular genetic study of 1765 cases with long-term follow-up. Am J Surg Pathol 2005;29:52-68.

[20] Michal M, Vanecek T, Sima R, Hes O, Mukensnabl P, Matoska J, et al. Mixed germ cell sex cord-stromal tumors of the testis and ovary. Morphological, immunohistochemical and molecular genetic study of seven cases. Virchows Arch 2006;448:612-22.